BNL-82144-2009-JA

DISTRIBUTIONS OF RAINDROP SIZES AND FALL VELOCITIES IN A SEMI-ARID PLATEAU CLIMATE: CONVECTIVE VS. STRATIFORM RAINS

Niu, S.[a]*, Jia, X.[a], Sang, J.[b], Liu, X.[a], Lu, C.[a], and Liu, Y.[c]

[a] Laboratory for Atmospheric Physics & Environment of China Meteorological Administration, Nanjing University of Information Science and Technology, Nanjing, P. R. China
[b] Ningxia Institute of Meteorological Science, Yinchuan, P. R. China
[c] Brookhaven National Laboratory, Upton, NY11973, USA
* Corresponding author: Laboratory for Atmospheric Physics & Environment of China Meteorological Administration Nanjing University of Information Science and Technology Nanjing, P. R. China; Tel.: 02558731385; fax: (+86)2557792648; E-mail: niusj@nuist.edu.cn.

Submitted for publication in
J. Applied Meteorol. Climatol.

March 2009

Environmental Sciences Department/Atmospheric Sciences Division

Brookhaven National Laboratory
P.O. Box 5000
Upton, NY 11973-5000
www.bnl.gov

Notice: This manuscript has been authored by employees of Brookhaven Science Associates, LLC under Contract No. DE-AC02-98CH10886 with the U.S. Department of Energy. The publisher by accepting the manuscript for publication acknowledges that the United States Government retains a non-exclusive, paid-up, irrevocable, world-wide license to publish or reproduce the published form of this manuscript, or allow others to do so, for United States Government purposes.

This preprint is intended for publication in a journal or proceedings. Since changes may be made before publication, it may not be cited or reproduced without the author's permission.

DISCLAIMER

This report was prepared as an account of work sponsored by an agency of the United States Government. Neither the United States Government nor any agency thereof, nor any of their employees, nor any of their contractors, subcontractors, or their employees, makes any warranty, express or implied, or assumes any legal liability or responsibility for the accuracy, completeness, or any third party's use or the results of such use of any information, apparatus, product, or process disclosed, or represents that its use would not infringe privately owned rights. Reference herein to any specific commercial product, process, or service by trade name, trademark, manufacturer, or otherwise, does not necessarily constitute or imply its endorsement, recommendation, or favoring by the United States Government or any agency thereof or its contractors or subcontractors. The views and opinions of authors expressed herein do not necessarily state or reflect those of the United States Government or any agency thereof.

Abstract

Number concentrations of raindrops with respect to sizes and fall velocities were measured with a Parsivel precipitation particle disdrometer in a field experiment conducted during July and August 2007 at a semi-arid continental site located in Guyuan, Ningxia Province, China (36°N, 106°16′E). Data from both stratiform and convective clouds are analyzed. Comparison of the observed raindrop size distributions shows that the increase of convective rain rates arises from the increases of both drop concentration and drop diameter while the increase of the rain rate in the stratiform clouds is mainly due to the increase of large drop concentration. Another striking contrast between the stratiform and convective rains is that the size distributions from the stratiform (convective) rains tend to narrow (broaden) with increasing rain rates. Statistical analysis of the distribution pattern shows that the observed raindrop size distributions from both rain types can be well described statistically by the Gamma distribution, especially for those of high rain rates. Examination of the raindrop fall velocity reveals the combined influences of turbulence and air density. The difference in air density leads to a systematic change in the drop fall velocity while different turbulent air motions likely cause the large spread of velocity at a certain raindrop diameter. The turbulence influence is strong for small drops, but decreases with increasing raindrop diameters.

Key words: raindrop size distributions, raindrop fall velocity, terminal velocity, Gamma distribution, semi-arid plateau

1. Introduction

As a key component of the hydrologic cycle, precipitation is critical for understanding the Earth's climate and predicting climate change as a result of human activities such as emission of greenhouse gases and aerosol particles into the atmosphere (Chahine 1992; Entekhabi et al. 1999). Precipitation processes need to be parameterized in global climate models because these processes occur over scales smaller than typical model grid sizes. Over the last few decades, increasing effort has been devoted to improving global satellite remote sensing of precipitation (Tokay 1996) and parameterization of precipitation processes in global climate models (Rotstayn 1997), and great progress has been made in both areas as a result. Despite the great progress, precipitation measurements and parameterization still suffer from large uncertainties, and much remains to be done.

As probably the most fundamental microphysical property of precipitation, knowledge of the raindrop size distribution (RSD) is essential for further improving remote sensing and parameterization of precipitation processes. Accurate knowledge of the RSD is important in telecommunications, precipitation scavenging of aerosol particles, soil erosion, and understanding precipitation physics as well (Uijlenhoet and Torres 2006). In particular, recent development in remote sensing techniques permits long-term retrievals of more RSD parameters and their vertical profiles over large areas (Bringi et al. 2003; Kirankumar et al. 2008). Such progress enhances our ability to monitor precipitation and provides powerful tools to investigate rainfall

microphysics, and at the same time, calls for more accurate assumptions regarding the spectral shape of RSDs. For example, studies have shown that RSDs vary both spatially and temporally, not only within a climatic regime but also within a specific rain type (Nzeukou et al. 2004). The wide RSD variability represents a major source of inaccuracy in rainfall estimation by remote sensing, and this is especially true for drops smaller than about 1.5 mm because of the limited sensitivity and accuracy of available remote sensing techniques (Williams et al. 2000). Our understanding of the RSD variation, esp., with different precipitation types is still far from complete, and more analyses of in situ measurements under a wide variety of climatic regimes are needed.

The raindrop fall velocity is an equally important quantity and closely related to the measurements of RSDs and various integral quantities such as rain rate. It has been long recognized that rainfall is often associated with various turbulent motions (e.g., updrafts and downdrafts) in and below clouds (Battan 1964), and that turbulent flows can exert substantial influence on the motion of raindrop (Pinsk et al 1996). However, the effect of turbulent motions on raindrop fall velocity has not been adequately addressed, and use of the terminal velocity measured in stagnant air (e.g., Gunn and Kinzer 1949) has been a common practice (Pruppacher and Klett 1998).

These issues regarding RSD and raindrop fall velocity stand out especially with precipitation over the semi-arid plateau in western China because of the scarcity of observational sites. To overcome these deficiencies, a field experiment targeting rainfall in the semi-arid plateau climate was conducted at Guyuan (36°N, 106°16′E),

Ningxia Province, China, to simultaneously measure RSDs and raindrop fall velocities with a Parsivel disdrometer. This paper examines the measurements collected during this experiment, with three foci: (1) characteristic comparison/contrast of the spectral shapes of RSDs from stratiform and convective rains and their variation with rain rates; (2) the analytical expression for describing the RSDs; and (3) raindrop fall velocities and the effects of air density and turbulent motions. The rest of the paper is organized as follows. Section 2 describes the field experiment. Section 3 presents RSD analyses. Section 4 examines the measurement of raindrop fall velocities. The major findings are summarized in Section 5.

2. Experiment Description

The field experiment was conducted at Guyuan (36°N, 106°16′E), Ningxia Province, China (Fig. 1). The site is located in a hilly-gully area of the Loess Plateau near the upper Yellow River, and falls in the semi-arid temperate continental climatic regime, with an annual mean temperature of 4.4-7.1ºC, annual mean cumulative rainfall of 478 mm, and mean annual evaporation of 1100-2000 mm.

Continuous measurements were taken from 17 July to 26 August 2007 to cover the raining season (from early July to late September). RSDs were measured with a Parsivel precipitation particle disdrometer manufactured by OTT Messtechnik, Germany. Löffler-Mang and Joss (2000) provided detailed description of this instrument. Briefly, the Parsivel probe is a laser-based optical disdrometer that can simultaneously measures both sizes and fall velocities of precipitation particles. The core element of the instrument is an optical sensor that produces a horizontal sheet of

light (180-mm long, 30-mm wide, and 1-mm high). The particle passing through the light sheet causes a decrease of signal due to extinction. The amplitude of the signal deviation is a measure of particle size, and the duration of the signal allows an estimate of particle fall velocity. Particles with diameters between 0.2 mm and 25 mm and fall velocities between 0.2 and 20 m $s^{-1}$are detectable by the instrument. The particle size and velocity are each categorized into 32 size and velocity bins, respectively, with different bin widths. The instrument was placed about 1.8 m above the ground. The disdrometer was calibrated daily. The time interval of each RSD measurement was 10 seconds. A total of 15893 instant RSD samples were collected from 30 precipitation events. Correction was taken for unrealistically low fall velocities resulting from sounding noise.

3. Raindrop Size Distributions

a. Comparison of RSDs in stratiform and convective rains

Precipitation is generally considered to be of two distinct types: stratiform and convective. Identification of RSD features with these two precipitation types is useful and important for numerous applications, e.g., in calculation of heating profiles, in development of rainfall retrieval algorithm, in precipitation parameterization for use in atmospheric models, and in deciphering microphysical processes (Tokay and Short 1996; Tokay et al. 1999; Rotstayn 1997). Generally speaking, vertical air velocities within clouds exhibit strong distinction between the two types of precipitation, with stratiform (convective) clouds having weaker (stronger) vertical motions. However, observations of vertical velocities are rare, and other features have been used to

identify different rain types. For example, stratiform rains are generally more uniform than convective rains. Existence of the bright band of radar reflectivity is thought to be associated with stratiform precipitation. Many previous studies have been mainly concerned with the partition between stratiform and convective periods during individual tropical rain event, and the appropriate partition approach is still a topic of hot debate (Atlas et al. 1999)

During this field experiment, we encountered 8 individual cases of stratiform rains and 21 cases of convective rains based on the radar observations and meteorological observations at the surface (Table 1), providing us a unique opportunity to examine the differences between individual events of stratiform and convective rains in a mid-latitude semi-arid climate. Surface observations of precipitating clouds and thunder characteristics show that the stratiform rains were often associated with nimbostratus or altostratus opacus whereas the convective rains are mainly concomitant with thunder and cumulonimbus capillatus, and cumulus congestus. Furthermore, about 81% of convective rains (mostly showers) happened in the afternoon due to local thermal instability. As an example, Figure 2 shows an image of the Plan Position Indicator (PPI) of a typical convective cell observed at 12:30 local time (Beijing Time, or BT hereafter) on July 26th, 2007.

Figure 3 compares the RSDs from the stratiform and convective rains obtained by averaging all the instant RSDs for each rain type sampled during the entire experimental period. Notably, on average, the convective rain tends to have more raindrops than the stratiform counterpart across most drop sizes, i.e., 0.8 mm < D <

7.5 mm. But, the stratiform rain has more small raindrops with D < 0.8 mm. The mean diameters for the stratiform and convective rains averaged over all the events are 0.52 mm and 0.91 mm, respectively. These values are comparable to those found by Niu (2002) in the same region. In comparison, much larger mean raindrop diameters for stratiform rains were observed in Beijing (0.95 mm, Liu et al. 2006) and Henan (0.76 mm, Hu et al. 2005), both of which belong to the temperate continental climate. The orographic effect and high evaporation rate may be responsible for the smaller mean diameter observed at Guyuan. For example, previous studies have showed that orographic lifting can create a large number of small raindrops by supplying enough condensates, resulting in RSDs with very small mean diameter (Rosenfeld and Ulbrich 2003). Furthermore, the convective RSD is much broader than the stratiform RSD, with the maximum raindrop diameters being 7.5 mm and 3.8 mm for the convective and stratiform rain, respectively.

b. RSD variation with the rain rate

To further discern the difference between the convective and stratiform rains, the observed RSDs of each rain type are further stratified into 6 or 7 classes according to their rain rates: $R \leq 2$ mm h^{-1}, $2 < R \leq 4$ mm h^{-1}, 4 mm $h^{-1} < R \leq 6$mm h^{-1}, 6 mm $h^{-1} < R \leq 10$ mm h^{-1}, 10 mm $h^{-1} < R \leq 20$ mm h^{-1}, 20 mm $h^{-1} < R \leq 40$ mm h^{-1}, and 40 mm $h^{-1} < R$. Figures 4a and b show the averaged RSDs of the different rain rate classes for the stratiform and convective rains, respectively. For the convective rains, both their maximum drop diameters and the number concentrations across all the diameter bins increase when rain rates increase, suggesting that increasing rain rates of the convective

rains arise from the combined increases of the drop concentration and raindrop diameters. The RSD variation with the rain rate for the stratiform rains is markedly different from that of the convective rains. The number concentration in the stratiform rains increases with increasing rain rates only when D > 1.3 mm; for the small drops with D < 1mm, the concentration decreases significantly with increasing rain rates (R > 10 mm h^{-1}). Also, unlike the convective rains, no increase in the maximum drop diameter is detected for the stratiform rains. These results indicate that the increase in the rain rate of the stratiform rains stems mainly from the increase of the large drop (D > 1.3 mm) concentration.

The differences between the convective and stratiform RSDs can be further seen from the relationships of the rain rate to the drop concentration, mean volume diameter, and relative dispersion of the RSD (defined as the ratio of the standard deviation to the mean diameter of the raindrop population). As shown in Fig. 5, at the same rain rate, the convective rains have values of volume-mean diameter and relative dispersion larger than those of the stratiform rains whereas the stratiform rains tend to assume relatively higher raindrop concentrations, consistent with what is shown in Fig.4. Furthermore, for the convective rains, raindrop concentration, mean-volume diameter and relative dispersion all increases as the rain rate increases. But, for the stratiform rains, although the volume mean diameter tends to increase with increasing rain rates, the relative dispersion tends to decreases. This striking distinction between the stratiform and convective rains will be examined in more detail in next section. The distinct dependences of volume-mean diameter and relative dispersion on the rain

rate further lead to the difference in the Z-R relationships between the convective and stratiform rains (Fig. 6).

c. Analytical function for describing RSDs

Over the last few decades, great effort has been devoted to finding the appropriate analytical expression for describing the RSD because of its wide utilities in many areas. For example, by analyzing previous measurements, Marshall and Palmer (1948) proposed the now famous Marshall-Palmer raindrop size distribution

$$N(D) = N_0 \exp(-\lambda D), \quad (1)$$

where D is the raindrop diameter, N(D) is the drop concentration per diameter interval, and N_o and λ are two empirical parameters. Since then the Marshall-Palmer distribution has become a milestone assumption in remote sensing of rainfall (Atlas 1973) and precipitation parameterization in atmospheric models (Kessler 1969). Later studies showed that although the exponential distribution tends to describe large-sample averaged raindrop size distributions well, instant spectra often deviate from it, and the Gamma distribution has been proposed as a first order generalization (Ulbrich 1983; Liu 1992, 1993; Tokay and Short 1996),

$$N = N_0 D^{\mu} \exp(-\lambda D), \quad (2)$$

where the spectral parameter μ is introduced to quantify the deviation of the spectral shape from the Marshall-Palmer distribution; the Gamma distribution reduces to the Marshall-Palmer distribution when μ equals 0. The Gamma size distribution has become a new standard assumption to replace the classic Marshall-Palmer distribution in many applications such as advanced remote sensing of precipitation (Tokay and

Atlas 1999) and multi-moment parameterization of precipitation (Ferreir et al. 1995).

Most previous studies on analytical RSDs have been based on empirical curve-fittings to individual measured RSDs. Since RSD are the end results of many complex processes that they can be considered to be stochastic in nature such as collision and coalescence (Jaw Leou-Jang 1966), statistical approaches that are applicable to a large number of individual RSDs are more desirable. Liu (1992) proposed such a simple statistical method based on the relationship between the skewness and kurtosis of the RSD to identify the statistical RSD pattern. Liu and Liu (1994) further applied a similar approach to study aerosol size distributions. Here we apply this approach to investigate if the statistical pattern of the RSDs follows the Gamma distribution, and if there are any pattern differences between the stratiform and convective RSDs.

Briefly, skewness (S) and kurtosis (K) of a RSD are defined by the following two equations:

$$S = \frac{\int (D_i - \overline{D})^3 \frac{N_i(D_i)}{N_t} dD}{\left[\int (D_i - \overline{D})^2 \frac{N_i(D_i)}{N_t} dD\right]^{3/2}}, \tag{3a}$$

$$K = \frac{\int (D_i - \overline{D})^4 \frac{N_i(D_i)}{N_t} dD}{\left[\int (D_i - \overline{D})^2 \frac{N_i(D_i)}{N_t} dD\right]^{2}} - 3, \tag{3b}$$

where D_i is the central diameter of the i-th bin, N_i is the number concentration of the i-th bin, and N_t is the total number concentration. For the Gamma distribution given by Eq. (2), it can be shown that

$$S = \frac{2}{\sqrt{1+\mu}}, \tag{4a}$$

$$K = \frac{6}{1+\mu}. \tag{4b}$$

Equations (4a) (4b) indicates that S = 2 and K = 6 for the commonly used Marshall-Palmer distribution with μ = 0. With the classical Marshall-Palmer distribution as a reference, the skewness and kurtosis deviation coefficients (C_s and C_k) are introduced such that

$$C_s = \frac{S^2}{4}, \tag{5a}$$

$$C_k = \frac{K}{6}. \tag{5b}$$

It is obvious that for the Gamma distribution, we have

$$C_s = C_k = \frac{1}{1+\mu}. \tag{6}$$

In the C_s-C_k diagram, each (C_s, C_k) pair represents an individual RSD; the general Gamma distribution with varying μ satisfies the diagonally straight line; the point (1, 1) represents the Marshall-Palmer distribution (Marshall and Palmer 1948) as a special Gamma function with μ=0.

Figures 7 shows the scatter plots of C_s and C_k calculated from the observed RSDs from the stratiform and convective rains. A few points are evident. First, despite some occasional departures, most of the points from both the convective and stratiform rains fall near the diagonal straight line of the Gamma distribution, confirming that the RSD patterns from both types of clouds well follow the Gamma

distribution statistically, with the correlation coefficients being 90.4% and 94.7% for the stratiform and convective rains, respectively. Second, the instantaneous pairs of C_s and C_k do not cluster around point (1, 1), suggesting that the Marshal-Palmer distribution is not suitable for describing most instantaneous RSDs. This finding is consistent with many previous studies (Liu 1992). Finally, the spectral shape varies substantially from one RSD to another, and the convective rains tend to have more RSDs with larger values of C_s and C_k compared to the stratiform rains.

To examine the dependence of the spectral shape on the rain rate, Fig. 8 further displays the scatter plot of C_s and C_k calculated from the RSDs averaged according to the rain rate classes shown in Fig. 4. Clearly, the rate-stratified RSDs of both rain types tend to statistically follow the Gamma distribution (C_s=C_k) as well, which is especially true when the rain rates are high（$R > 6$ mm h^{-1}). The remarkable contrast between the stratiform and convective rains in the variations of (Cs, Ck) with the rain rate is noteworthy: When the rain rate increases, C_s and C_k decrease away from the Marshall-Palmer point (1, 1) for the stratiform rains, but increases toward the Marshall-Palmer point (1, 1) for the convective rains. This contrast is in general agreement with that of the variation of the relative dispersion with the rain rate shown in Fig. 5.

4. Raindrop Fall Velocity

a. General feature

In addition to drop sizes, the Parsivel disdrometer measures drop fall velocities as well (Löffler-Mang and Joss 2000). Figures 9a and b shows the observed mean

number concentration as a function of the drop diameter and the fall velocity for the stratiform and convective rains, respectively. Also shown as a reference (black solid curve) is the laboratory measurements by Gunn and Kinzer (1949) of the terminal velocities under the standard atmospheric conditions at sea level (air pressure of 1013 mb, temperature of 20 ^{0}C, and relative humidity of 50%). Consistent with the RSDs shown in Fig.3, raindrops in the stratiform rain concentrate in the range of fall velocities of 2-4 m s^{-1} and then decrease sharply with increasing fall velocities while the raindrops in the convective rain peak at higher velocities (4-6 ms^{-1}) and decrease with increasing velocities much more slowly. Besides these differences, the stratiform and convective rains share some similarities too. First, on average, the observed drop fall velocities for both rain types tend to be higher than the corresponding Gunn-Kinzer terminal velocities obtained under the standard sea-level conditions. Second, there are large spreads in the drop fall velocities at virtually all the drop diameters, with the convective rains having an even larger spread than that the stratiform rains. Similar features have been previously reported in rare studies of *in situ* measurements of drop fall velocities (Donnadieu 1980; Hosking and Stow 1991; Löffler-Mang and Joss 2000). In the next two sub-sections, the physical mechanisms underlying the large spread in the measured fall velocities, and the systematic discrepancy between the measured fall velocities and the Gunn-Kinzer terminal velocities will be examined in detail.

b. Air density effect and systematic discrepancy

The classical Gunn-Kinzer measurement of the drop terminal velocity was

conducted under the standard atmospheric conditions at sea level, with the air density of 1.23 kg m^{-3}. However, the air properties at Guyuan during the observational period are markedly different, with the altitude of 1753 m above sea level, mean pressure of 819.3 hPa, and mean air density of 0.97 kg m^{-3}. It is expected that the lower air density at Guyuan will result in a terminal velocity larger than the corresponding Gunn-Kinzer terminal velocity, other things being the same (Pruppacher and Klett 1996).

Many studies have been attempted to extrapolate the Gunn-Kinzer measurements to other atmospheric conditions, and to quantify the effect of air density on the drop terminal velocity (Battan 1964; Foote and du Toit 1969; Atlas 1973; Beard 1976, 1977). In particular, Mitchell (1996) presented a general, semi-theoretical framework by coupling the Abraham (1970) conceptual model to the power-law relationship between the Reynolds number and Best number. The Mitchell formulation not only accounts for the effect of air density but also is easy to grasp mathematically and physically. In view of these advantages of the Mitchell formulation, below we apply this formulation to evaluate the contribution of the air density difference to the systematic discrepancy between the observed drop fall velocity and the Gunn-Kinner terminal velocity.

Briefly, the mass and area-dimensional relationships can be described by power laws such that,

$$m = \alpha D^{\beta}, \tag{7}$$

$$A = \gamma D^{\sigma}, \tag{8}$$

where m, A and D are the mass, area and maximum dimension of the particle respectively; α, β, γ, and σ are the empirical parameters depending on particle shapes. The Reynolds and Best numbers are given by

$$R_e = \frac{\rho_a D V_t}{\eta}, \tag{9a}$$

$$X = \frac{2\alpha g \rho_a D^{\beta+2-\sigma}}{\gamma \eta^2}, \tag{9b}$$

where g is the gravitational constant, η is the air dynamic viscosity, and ρ_a is the air density. Over a certain range of X, the relationship between Re and X can be approximated by a power law expression (Knight and Heymsfield 1983; Heymsfield and Kajikawa 1987)

$$\mathrm{Re} = aX^b, \tag{10}$$

where the empirical coefficients a and b depends on the range of X. A combination of Eqs. (9) and (10) leads to the general expression for the terminal velocity

$$V_t = a\eta^{1-2b}\left(\frac{2\alpha g}{\gamma}\right)^b \rho_a^{b-1} D^{b(\beta+2-\sigma)-1}. \tag{11}$$

Under the assumption that the parameters α, β, γ, and η are independent of the air density or simply a constant, Eq. (11) can be simplified as

$$V_t = V_0\left(\frac{\rho_a}{\rho_0}\right)^{b-1}, \tag{12}$$

where V_0 represents the terminal velocity in the standard atmosphere at the sea level, say the Gunn-Kinzer terminal velocity. Equation (12) reveals that the effect of air density is determined by the value of b. For convenience, Table 2 summaries the values of b for the two ranges of X applicable to the rain drops encountered during the

field experiment. The values of b = 0.6 and 0.5 lead to the correction factors of $\left(\frac{\rho_a}{\rho_0}\right)^{-0.4}$ and $\left(\frac{\rho_a}{\rho_0}\right)^{-0.5}$ for $585 < X \le 1.56\times10^5$ and $1.56\times10^5 < X \le 10^8$, respectively. It is interesting to note that these semi-theoretical correction factors are very close to the empirical ones suggested in Foote and du Toit [1969, $\left(\frac{\rho_a}{\rho_0}\right)^{-0.4}$] and Atlas [1973, $\left(\frac{\rho_a}{\rho_0}\right)^{-0.5}$], revealing that these two previous correction factors actually hold over different ranges of X or drop diameters.

Using Eq. (12) with the proper values of b, air densities and V_0, we calculated the theoretical dependence of the terminal velocity on the drop diameter corrected for the effect of air density at Guyuan. The result is shown as the red solid curve in Fig. 9. It is evident that compared to the Gunn-Kinzer terminal velocity, correction for the effect of air density brings the terminal velocities much closer to the observed drop fall velocities. The improved agreement suggests that the lower air density at Guyun is (at least partly) responsible for the systematic discrepancy between the terminal velocities and the Parsivel-measured drop fall velocities. The difference between the air densities at Guyuan and at the standard sea level leads to a percent difference of 10 to 12% in the terminal velocity, depending on the value of b (0.6 or 0.4).

c. Turbulence effect and large spread

The difference in air density can explain away (some) systematic deviation of the Parsivel-measured fall velocity from the Gunn-Kinzer terminal velocity, but it leaves unresolved the large spread in the measurement of the instant drop fall velocity. It has been long recognized that complex air motions, esp., updrafts and downdrafts, often

accompany natural rainfall, leading deviations in the shape, velocity and trajectory of falling raindrops from those in still air where the dependence of terminal velocity on raindrop diameter is developed (Kinnel 1976; Donnadieu 1980). For example, in probably the only existing investigation of the Parsivel-measured drop velocities, Löffler-Mang and Joss (2000) found similar spreads in their measured relationship between the drop fall velocity and terminal velocity, and attributed the spread to air turbulence and instrumental errors. However, the limited previous studies have been largely qualitative, lacking rigorous investigation. Here we will further the previous studies to examine this issue of spread and the effect of turbulent motions in a more quantitative way.

Without loss of generality, the fall velocity (V) of a raindrop measured by the Parsivel probe can be regarded as a combination of the terminal velocity in still air (V_t) and a component resulting from turbulent air motions and/or measurement errors (V_m):

$$V = V_t + V_m . \qquad (13)$$

According to Eq. (13), a positive V_m (e.g., caused by a downdraft) will make the drop fall faster than the still-air terminal velocity; on the contrary, a negative V_m (e.g., caused by an updraft) will do just the opposite. It is well known that clouds are areas of enhanced turbulence and rainfall which are associated with a complex mixture of upward and downward air motions of various scales. The large spread of the measurements at both sides of the terminal velocity curves shown in Fig. 9 seems compatible with the notion of nearly random collections of downdrafts and updrafts

for the stratiform and convective rains examined. A wider spread for the convective rains implies stronger vertical motions compared to their stratiform counterparts, which is consistent with our general understanding of both rain types. The velocity deviation, which is the difference between the Parsivel-measured fall velocity and the corresponding terminal velocity, measures the total effect from the other factors,,

$$\Delta V = V - V_t = V_m . \quad (14)$$

Furthermore, if all the factors that affect V_m were completely random, the mean of Eq. (14) over an ensemble of samples would lead to

$$\overline{(\Delta V)} = \bar{V} - V_t = 0 . \quad (15)$$

Equation (15) also indicates that a perfect random distribution of V_m will result in the average of many instantaneous measurements being equals to the corresponding terminal velocity corrected for the effect of air density. To examine if Eq. (15) holds or if there are any systematic differences between the drop fall velocity and the terminal velocity in addition to that caused by the difference in air density discussed in Section 4b, Fig. 10 shows the mean velocity deviation against the drop diameter for the stratiform and convective rains at Guyuan. Obviously, the mean deviation velocities are positive for small drops with diameters <1.2mm, indicating that the Parsivel-measured fall velocities are higher than the corresponding terminal velocities.. The overestimation reaches maximum for small raindrops, decreases sharply when the drop diameter increases from 0.2 to ~ 1.5 mm. On the contrary, the mean deviation velocities are negative for large drops.. This negative velocity deviation could stem from the occurrence of a significant updraft surrounding drops

over large sizes, extremely in convective rains. More research is necessary to ascertain this anomaly.

To assess the effect of turbulent motions relative to increasing terminal velocity with increasing drop diameters, Fig. 11 further shows relative velocity deviation which is the root-mean-square velocity deviation normalized by the corresponding terminal velocity. The Parsivel probe can overestimate the terminal velocity by up to 150% for small drops of 0.3 mm diameter; the overestimation then decreases sharply with increasing drop diameters, to 10% at 1 mm diameter, and stays approximately at 10% level after that. The 10% deviation is comparable to that caused by the different air density in magnitude, implying that the average effect of turbulent motions is about two times larger than that of the air density. Still larger effect of turbulent motions is on the instant Parsivel-measured raindrop fall velocity.

The particularly large mean velocity deviation for small raindrops is noteworthy. Löffler-Mang and Joss (2000) regarded instrumental limitations such as quantization, threshold, and drop slashing on the housing as the likely reasons for it. Drop slashing and subsequent fragmentation was also suggested to produce unrealistically low fall velocities by Krajewski et al. (2006). On the other hand, Pinsky and Khain (1996) demonstrated through numerical simulations that wind shear of turbulent flows and the inertial acceleration of particles in atmospheric turbulence can result in substantial drop velocity deviations from the air velocity. Furthermore, the result shown in Fig. 12 appears to qualitatively resemble the variation of the relative turbulence-induced velocity deviation with the drop diameter shown in Fig. 17 of Pinsky and Khain

(1996). These results qualitatively agree with Pinsky and Khain's (1996) model simulation results. Therefore, we cannot totally rule out the possibility of atmospheric turbulence inducing some fall velocity vertical for small drops. The potential effect of falling raindrops on turbulent motions adds another layer of complexity to this issue, and more research is needed to ultimately resolve it.

5. Conclusion

A field experiment was conducted at a site located in the regime of semi-arid temperate plateau climate. A total of 30 rainfall events were sampled and classified into 8 stratiform and 21 convective rains. A total of 15893 joint raindrop size and fall-velocity distributions measured with a Parsivel disdrometer are analyzed to discern the similarity and difference between stratiform and convective rains, to determine the statistical pattern of the raindrop size distribution, and to examine the mechanisms that affect raindrop fall velocities. Comparison of the type-averaged raindrop size distributions shows that the convective rains have more raindrops with drop diameters larger than 0.8 mm than the stratiform rains whereas the opposite is true for raindrops smaller than 0.8 mm. The convective raindrop size distribution is also broader than the stratiform raindrop size distribution. Further comparison of the raindrop size distributions stratified according to rain rates reveals that for the convective rains the increase of rain rate arises from the combined increases of drop concentration and maximum diameter while for the stratiform rains rain rate increases are mainly due to the increase of large drop concentration.

It is shown by use of an approach based on the relationship between the deviation

coefficients of skewness and kurtosis that the instantaneous 10-s raindrop size distributions from both the convective and stratiform rains can be well described statistically by the Gamma distribution. Application of the same approach to the raindrop size distributions averaged according to rain rates further reveals a striking contrast of the variation of spectral shape with the rain rate between the stratiform and convective rains: The stratiform and convective raindrop size distributions tend to narrow and broaden with increasing rate rates, respectively.

Three characteristic features of the Parsivel-measured raindrop fall velocities are found: (1) on average, the former is systematically larger than the classical Gunn-Kinzer terminal velocity obtained at the standard sea-level; (2) there is substantial spread in the instantaneous Parsivel-measured raindrop fall velocities across all the raindrop sizes; (3) the spread for the convective rain appears wider than that for the stratiform rain. The effects of air density and turbulent motions on raindrop fall velocities are examined rigorously as plausible reasons. It is shown that the measurement site assumes an air density lower than that of the standard sea level. By using the Mitchell semi-theoretical formulation for the terminal velocity, a new expression is derived that accounts for the effect of air density. Application of this new expression with the air density at the experiment site suggests that the lower air density results in a terminal velocity about 10% systematically larger than the Gunn-Kinzer terminal velocity measured at the standard sea level. Correction for this air density effect moves of the terminal velocity much closer to the mean Parsivel-measured raindrop fall velocity. Theoretical analysis shows that the spread of

the mean measured drop velocities are likely associated with nearly random mixture of updrafts and downdrafts, and that the larger spread for the convective rain arises likely from strong fluctuations of vertical motions. Analysis of the dependence of the relative velocity deviation on the raindrop diameter further suggests that the Parsivel probe can overestimate the terminal velocity by up to 150% for small drops of 0.3 mm diameter; the overestimation then decreases sharply with increasing drop diameters, to 10% at 1 mm diameter, and stays approximately at 10% level after that. Evaluation of the relative contributions to the drop fall velocity indicates that the average effect of turbulent motions is about two times larger than that of the air density, and turbulent motions are likely the main reason for the large spread in the instant Parsivel-measured raindrop fall velocity.

Acknowledgements

This study is mainly supported by the Chinese National Science Foundation under Grant No.40537034 “Observational Study on Rainfall Physical Processes and Seeding Effect of Stratiform Cloud” and by the Ministry of Science and Technology of China under No.2006BAC12B00010107 “Critical Technology and Equipment Development in Weather Modification.” Y. Liu is supported by the ARM program of the U. S. Department of Energy. The authors thank Drs. Mitchell at DRI and Heymsfield at NCAR for their stimulating suggestions. The authors also thank our colleagues at the Laboratory for Atmospheric Physics& Environment of China Meteorological

Administration and Ningxia Institute of Meteorological Science for their support during the field experiment.

References

Abraham F. F., 1970: Funtional dependence of drag coefficient of a sphere on Reynolds number. *Phys. Fluids.*,13, 2194-2195.

Atlas, D., 1973: Doppler radar characteristics of precipitation at vertical incidence. *Rev. Geophys., Space Phys.* 11, 1-35.

Atlas, D., et al., 1999: Systematic variation of drop size and radar-rainfall relations. *J. Geophys. Res.*, D104, 6155-6169.

Battan, L. J., 1964: Some observations of vertical velocities and precipitation sizes in a thunderstorm. *J. Appl. Meteorol.*, 33, 415-420.

Battan, L. J., and J. B. Theiss, 1970: Measurement of vertical velocities in convective clouds by means of Pulsed-Doppler Radar. *J. Atmos. Sci.*, 27, 293-298.

Beard, K.V., 1976: Terminal velocity and shape of cloud and precipitation drops aloft. *J. Atmos. Sci.*, 33, 851-864.

Chahine, M., 1992: GEWEX: The global energy and water cycle experiment: EOS Trans. *Amer. Geophys.*, Union 73, 901–907.

Chen, B. J., Li, Z. H., Liu, J. C, 1998: Model of raindrop size distribution in three types of precipitation. *Acta Meteorologica Sinica.*, 56, 506-512.

Donnadieu G., 1980: Comparison of results obtained with the VIDIAZ spectropluviometer and the Joss–Waldvogel rainfall disdrometer in a “rain of a thundery type.”. *J. Appl. Meteor.*, 19, 593–597.

Entekhabi, D., Asrar, G. R., Betts, A. K., Beven, K. J., Bras, R. L., Duffy, C. J., Dunne, T., Koster, R. D., Lettenmaier, D. P., McLaughlin, D. B., Shuttleworth, W. J., van Genuchten, M.T., Wei, M.-Y., Wood, E. F., 1999: An agenda for land surface hydrology research and a call for the second international hydrological decade. *Bull. Amer. Meteorol.* Soc., 80, 2043–2058

Ferrier, B. S., W. K. Tao, and J. Simpson, 1995: A double-moment multiple-phase four class bulk ice scheme. Part I. *J. Atmos. Sci*., 52, 1001-1033.

Foote, G. B. and P.S. du Toit, 1969 : Terminal velocity of raindrops aloft. *J. Appl. Meteorol*., 8, 49-253.

Gong, F. J., He, Y. J., 2007: Characteristics of raindrop size distributions of northeast cold vortex precipitation in China. *Scientia Meteorologica Sinica*, 27, 365-374.

Gunn, R., Kinzer, G. D., 1949: The terminal velocity of fall for water drops in stagnant air. *J. Met.* 6, 243-248

Heymsfield, A., and M. Kajikawa, 1978: An improved approach to calculating terminal velocities of plate-like crystals and grauple. *J. Atmos. Sci.*, 44, 1088-1099

Hosking, J. G., and C. D. Stow, 1991: Ground-based measurements of raindrop fall speeds. *J. Atmos. Oceanic Technol.*, 8, 137-147.

Jaw Leou-Jang 1966

Kessler, E, 1969: On the distribution and continuity of water substance in atmospheric circulation. *Meteorol. Monogr.*, 10,32,84.

Kinnell, P. I. A., 1976: Some observations of the Joss-Waldvogel rainfall disdrometer. *J. Appl. Meteor.*, 15, 499-502.

Kirankumar, N. V. P., Rao, T. N., Radhakrishna, B., Rao D. N., 2008: Statistical characteristics of raindrop size distribution in Southwest Monsoon season. *J. Appl. Meteorol. Climat.*, 47, 576-590.

Knight N. C., and A. J. Heymsfield, 1983: Mearsurement and interpretation of hailstone density and terminal velocity. *J. Atmos. Sci*., 40, 1510-1516

Krajewski, W. F., Kruger, A., Caracciolo, C., Golè, P., Barthes, L., Creutin, J.D., Delahaye, J.Y., Nikolopoulos, E.I., Ogden, F., Vinson, J.P., 2006: DEVEX-disdrometer evaluation experiment: Basic results and implications for hydrologic studies. *Adv. Water Resource*, 29, 311-325.

Li, J., You, L. G., Hu, Z. J., 2006: Analysis on raindrop size distribution characteristics of Maqu Region in upper reach of Yellow River. *Plateau Meteorology,* 25, 942-949.

Liu, H. Y., L. H., 2006: Characteristics of rain from stratiform versus convective cloud based on the surface raindrop data. *Chinese Journal of Atmospheric Sciences*, 30, 693-702.

Liu, Y. G., 1991: The application of skewness and kurtosis to the studies on particle distribution. *Journal of Atmosphere,* 17, 9-15.

Liu, Y. G., Chen, W. K., Liu, G. Z., 1993: Investigation of aerosol particle size spectra-A simple statistical method. *Acta Scientiae Circumstantiae*, 13, 22-30.

Löffler-Mang, M., Joss J., 2000: An optical disdrometer for measuring size and velocity of hydrometeors. *J. Atmos. Ocean. Technol*., 17, 130-139.

Marshall, J.S., Palmer, W.M., 1948: The distribution of raindrops with size. *J. Meteorol.*, 5, 165-166.

Mitchell, D. L., 1996: Use of mass- and area-dimensional power laws for determining precipitation particle terminal velocities. *J. Atmos. Sci.*, 53, 1710-1723.

Niu Shengjie, An Xialan, San Jianren, 2002: Observational research on physical feature of summer raindrop size distribution under synoptic systems in Ningxia. Plateau Meteorology, 21, 37-44.

Nzeukou, A., Sauvageot, H., Ochou, A. D., Kebe, C. M. F., 2004: Raindrop size distribution and radar parameters at Cape Verde. J. Appl. Meteorol., 43, 90-105.

Pinsky, M. B. and Khain, A. P., 1996: Simulations of drop fall in a homogeneous

isotropic turbulent flow. Atmos. Res., 40, 223-259

Pruppacher, H.R., Klett, J.D., 1998: Microphysics of clouds and precipitation. *Kluwer Academic,* 954 pp.

Rosenfeld, D., Ulbrich C. W., 2003: Cloud Microphysical Properties, Processes, and Rainfall Estimation Opportunities, *Meteorological Monographs*，30, 237pp.

Rotstayn, L. D., 1997: A physically based scheme for the treatment of stratiform clouds and precipitation in large-scale models. I: Description and evaluation of the microphysical processes. Q. J. R. Meteorol. Soc., 123, 1227-1282.

Sauvageot, H., Lacaux, J.P., 1995: The shape of averaged drop size distributions. *J. Atmos. Sci.*, 52, 1070–1083.

Sheppard, B. E., and Joe, P. I., 1994: Comparison of raindrop size distribution measurements by a Joss-Waldvogel disdrometer, a PMS 2DG spectrometer, and a POSS Doppler Radar. *J. Atmos. Ocean. Technol.*, 11, 874-887.

Shi, A. L., Zheng, G. G., Huang, G., 2004: Characteristics of raindrop spectra of stratiform cloud precipitation in autumn 2002 in Henan Province. *Journal of Atmosphere,* 8, 12-17.

Steiner, M., Smith, J.A., Uijlenhoet, R., 2004: A microphysical interpretation of radar reflectivity–rain rate relationships. *J. Atmos. Sci.*, 61, 1114–1131.

Tokay, A., and Short, D. A., 1996: Evidence from tropical raindrop spectra of the

origin of rain from stratiform versus convective clouds, *J. Appl. Meteor.*, 35, 355–371.

Tokay, A., and Atlas, D., 1999: Rainfall microphysics and radar properties: analysis methods for drop size spectra. *J. Appl. Meteor.*, 37, 912-320.

Uijlenhoet, R., Smith, J. A. and Steiner, M., 2003: The microphysical structure of extreme precipitation as inferred from ground-based raindrop spectra, *J. Atmos. Sci.,* 60, 1220-1238.

Uijlenhoet, R. and Torres, D. S., 2006: Measurement and parameterization of rainfall microstructure. *J. Hydrol*. 328, 1-7.

Ulbrich, C. W., 1983: Natural variations in the analytical form of t he raindrop size distribution. *J. Climate Appl. Meteorol.*, 5, 1764-1775.

Williams, C. R., P. E. Johnston, and K. S. Gage, 2000: Cluster analysis techniques to separate air motion and hydrometeors in vertical incident profiler observations. *J. Atmos. Oceanic Technol.,* 17, 949–962.

Figure Captions

Fig. 1. Geographic illustration of the experiment site and its surroundings. The white curve encircles the Ningxia Province.

Fig.2. PPI displays of velocity (a) and intensity (b) of radar echoes observed in Guyuan (marked with a dot and Chinese) at 1230 BJT on July 26th, 2007.

Fig. 3. Average raindrop size distributions for the stratiform and convective rains from the entire dataset.

Fig. 4. Raindrop size distributions averaged according to different rain rates for the stratiform (a) convective (b) rains.

Fig.5. Relationship to the rain rate of the drop concentration (red and left axis, volume-mean diameter (blue and first right axis), and relative dispersion (green and second right axis) for the stratiform (solid dots) and convective rains (crosses).

Fig. 6. Relationship between the radar reflectivity and rain rate for the stratiform (solid dots) and convective rains (crosses). The equations are the curve-fitting results.

Fig. 7. C_s-C_k scatter plot of the instantaneous raindrop size distributions for the stratiform rain (black solid dots) and convective rain (red crosses). Each point represents one 10-s observed raindrop size distributions. The straight line presents the C_s-C_k relation of the gamma function.

Fig. 8. C_s-C_k scatter plot for the raindrop size distributions averaged according to different rain rates. The red and black colors denote the convective and stratiform rains, respectively; the circle sizes reflect the rain rates, with a smaller circle corresponding to a lower rain rate.

Fig. 9. Number concentration distribution (color shadings) as a function of the drop diameter and raindrop fall velocity for the stratiform rains (a) and convective rains (b) The black curve (V_0) in each panel shows the empirical relationship between diameter and velocity of Atlas (1973) after the measurements from Gunn and Kinzer (1949): $v=9.65-10.3e^{-0.6D}$. The blue curves are the simulation of Mitchell's terminal velocity considering the air density effect in Guyuan. The red curves are the simulation of Beard's (1976) terminal velocity considering the air density effect in Guyuan.

Fig. 10. Dependence of the mean velocity deviation on the raindrop diameter for the stratiform (solid circle) and convective (crosses) rains.

Fig. 11. Dependence of the relative mean velocity deviation on the raindrop diameter for the stratiform (solid circle) and convective (crosses) rains.

Table 1. Summary of observed rainfall events
H is the cumulative rainfall measured by surface station; *C* and *S* refer to convective and stratiform precipitation, respectively.

Events	Number of samples	*H* （mm）	Rain type	$\overline{R}$ (mm h^{-1})
17 Jul a	356	22.4	*C*	6.16
17 Jul b	1527		*C*	4.93
18 Jul a	197	0.5	*S*	0.90
18 Jul b	100		*S*	0.47
19 Jul	2116	4.1	*S*	0.94
20 Jul	2956	5.6	*S*	0.87
21 Jul	217	0.6	*C*	1.49
22 Jul	29	0.0	*C*	1.28
24 Jul a	27	0.4	*C*	1.15
24 Jul b	76		*C*	1.83
26 Jul a	140	1.5	*C*	1.07
26 Jul b	45		*C*	7.69
27 Jul a	425	2	*C*	1.80
27 Jul b	64		*C*	0.29
29 Jul	95	0.2	*C*	0.91
31 Jul a	35	0.0	*C*	0.33
31 Jul b	14		*C*	0.45
3 Aug	45	0.7	*C*	3.89
4 Aug	286	1.2	*C*	1.79
5 Aug	7	0.0	*C*	1.83
6 Aug a	109	6.1	*C*	23.30
6 Aug b	16		*C*	0.34
8 Aug	1979	16.7	*C*	3.62
9 Aug	64	0.7	*S*	0.06
12 Aug	74	1.4	*C*	9.83
25 Aug	644	11.9	*C*	7.90
26 Aug a	375		*S*	0.63
26 Aug b	3863	8.4	*S*	0.85
26 Aug c	14		*S*	0.18

Table 2. Summary of terminal velocity expressions.

b is the empirical coefficients b of power law of Re and X. ρ_a is the air density. ρ_0 is the air density at the standard sea level. X is the Best numbers.

Terminal Velocity (V_t)	b	Best Numbers (X)
$V_t = (9.65 - 10.3e^{-0.6D}) * \left(\frac{\rho_a}{\rho_0}\right)^{0.638-1}$	0.638	$585 < X \leq 1.56 * 10^5$
$V_t = (9.65 - 10.3e^{-0.6D}) * \left(\frac{\rho_a}{\rho_0}\right)^{0.499-1}$	0.499	$1.56 * 10^5 < X \leq 10^8$

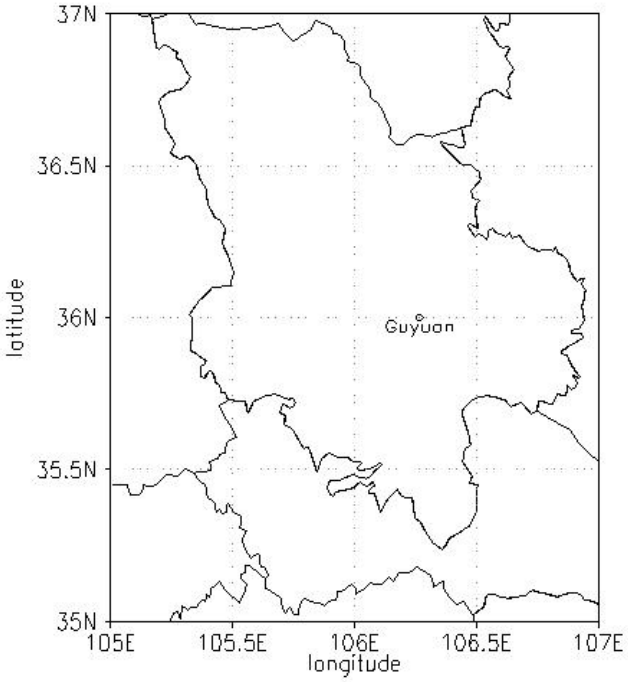
37N
36.5N
36N
35.5N
35N
latitude
Guyuan
105E
105.5E
106E
106.5E
107E
longitude

Figure 1

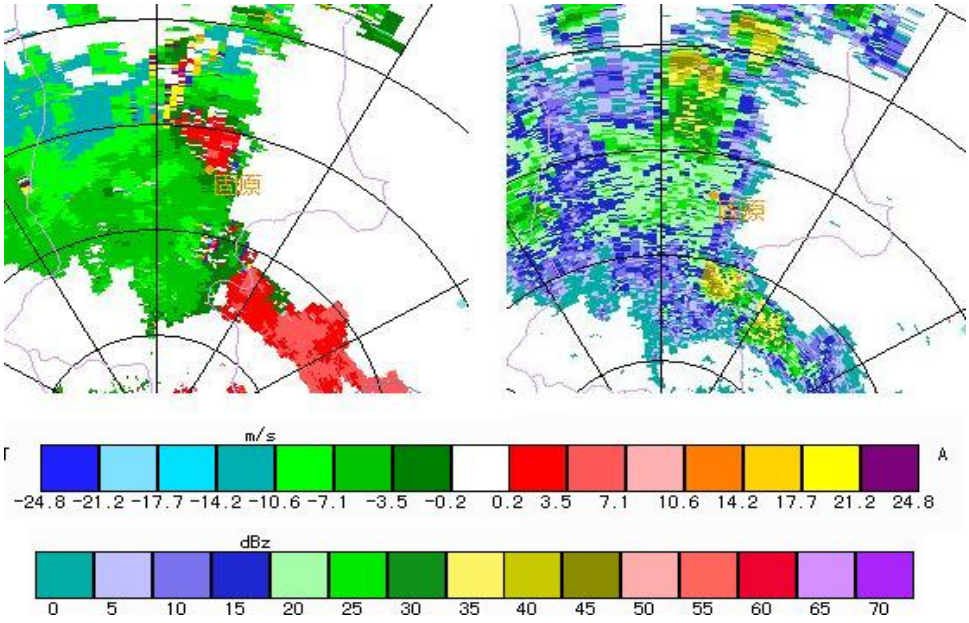
固原
固原
m/s
-24.8 -21.2 -17.7 -14.2 -10.6 -7.1 -3.5 -0.2 0.2 3.5 7.1 10.6 14.2 17.7 21.2 24.8
dBz
0 5 10 15 20 25 30 35 40 45 50 55 60 65 70

Figure 2

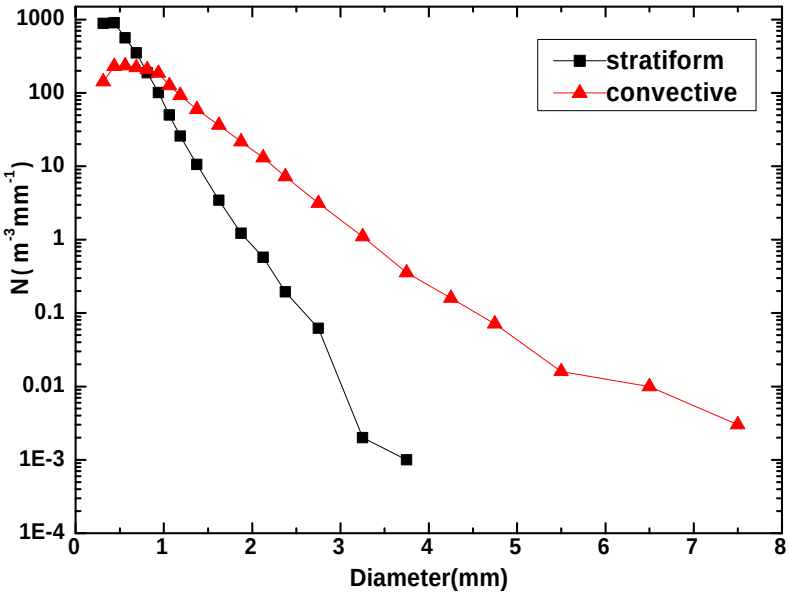
stratiform
convective
N (m-3 mm-1)
Diameter(mm)
1000
100
10
1
0.1
0.01
1E-3
1E-4
0
1
2
3
4
5
6
7
8

Figure 3

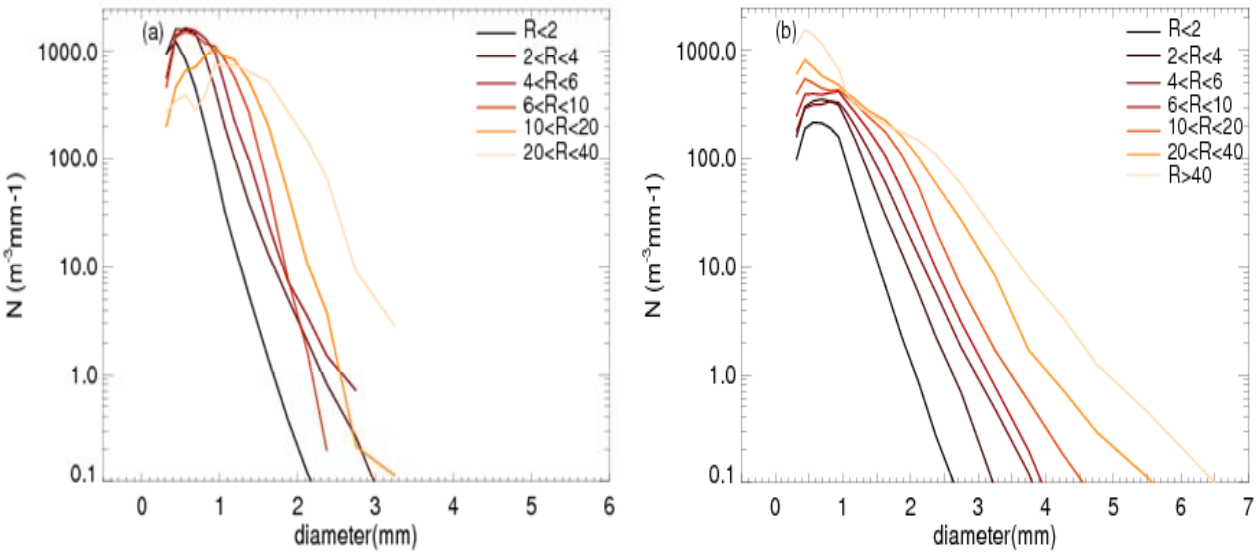
(a)
R<2
2<R<4
4<R<6
6<R<10
10<R<20
20<R<40
1000.0
100.0
10.0
1.0
0.1
N (m-3mm-1)
0
1
2
3
4
5
6
diameter(mm)
(b)
R<2
2<R<4
4<R<6
6<R<10
10<R<20
20<R<40
R>40
1000.0
100.0
10.0
1.0
0.1
N (m-3mm-1)
0
1
2
3
4
5
6
7
diameter(mm)

Figure 4

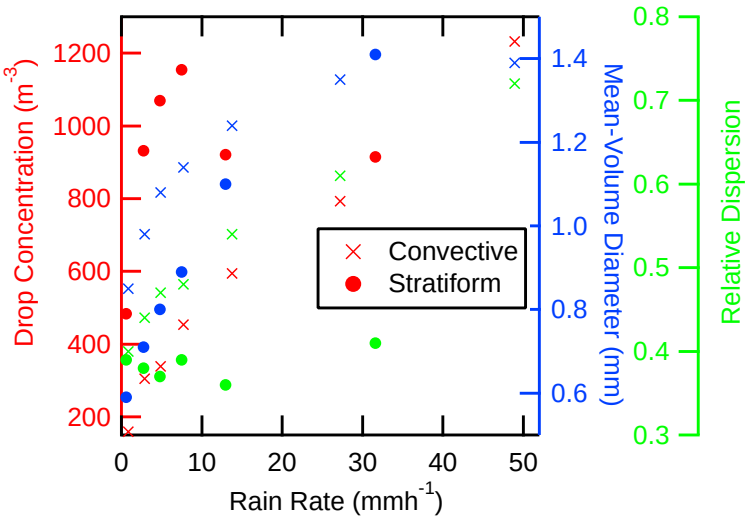
Drop Concentration (m-3)
1200
1000
800
600
400
200
0
10
20
30
40
50
Rain Rate (mmh-1)
1.4
1.2
1.0
0.8
0.6
Mean-Volume Diameter (mm)
0.8
0.7
0.6
0.5
0.4
0.3
Relative Dispersion
Convective
Stratiform

Figure 5

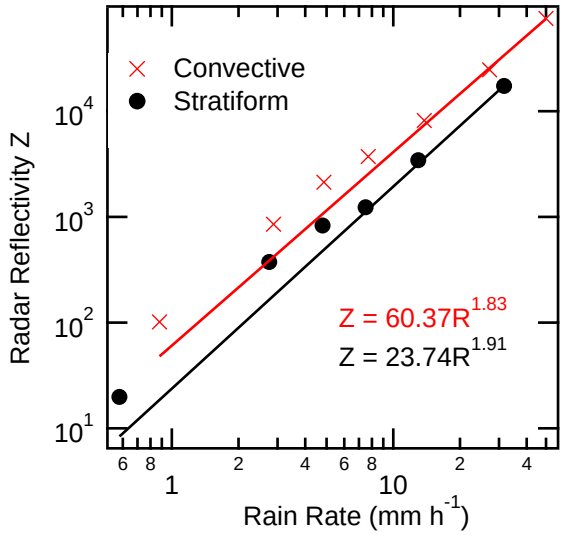
Convective
Stratiform
Z = 60.37R^1.83
Z = 23.74R^1.91
Radar Reflectivity Z
Rain Rate (mm h^-1)
10^4
10^3
10^2
10^1
6 8
1
2
4
6 8
10
2
4

Figure 6

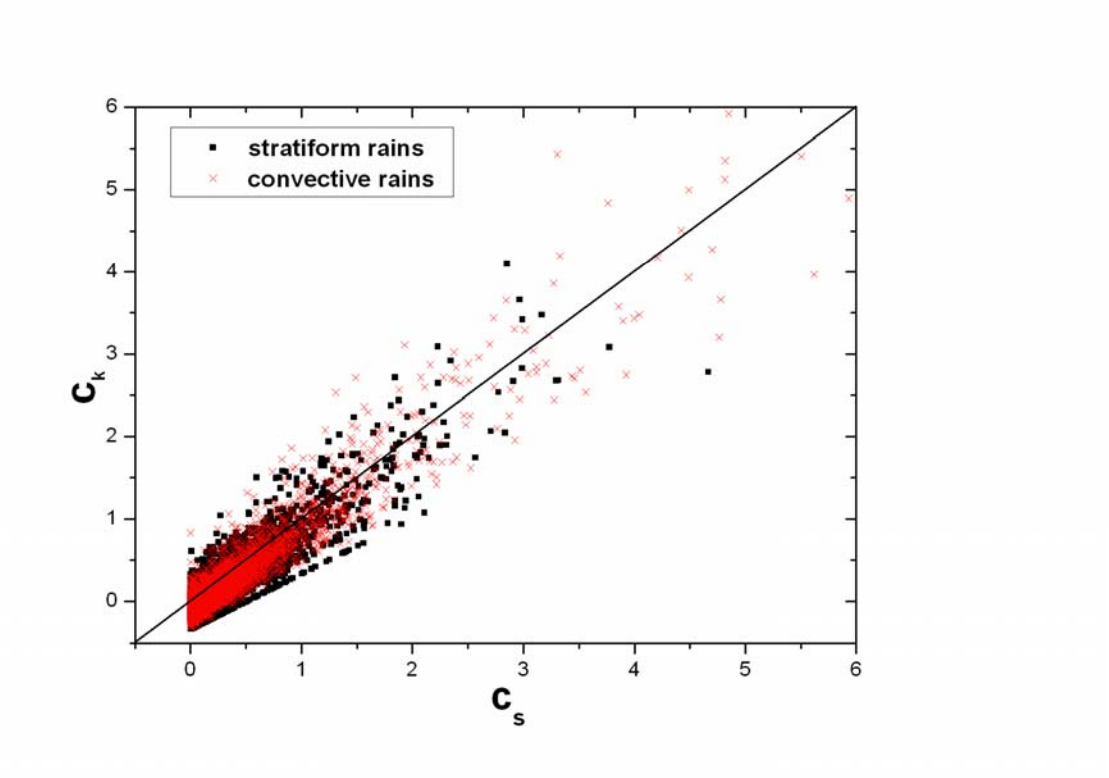

Figure 7

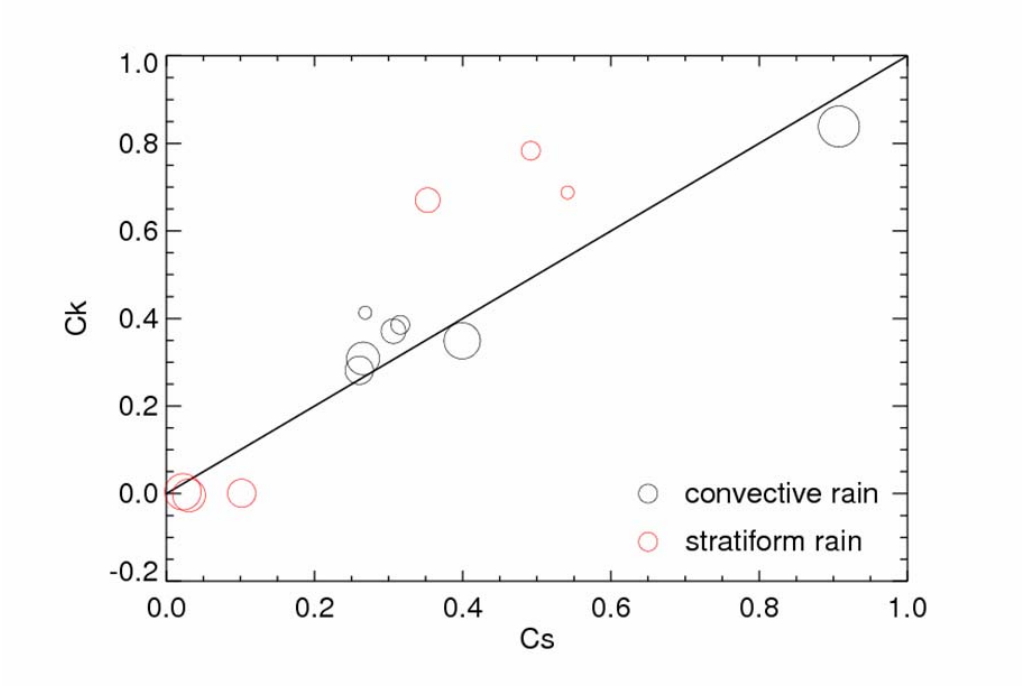
1.0
0.8
0.6
0.4
0.2
0.0
-0.2
Ck
0.0
0.2
0.4
0.6
0.8
1.0
Cs
convective rain
stratiform rain

Figure 8

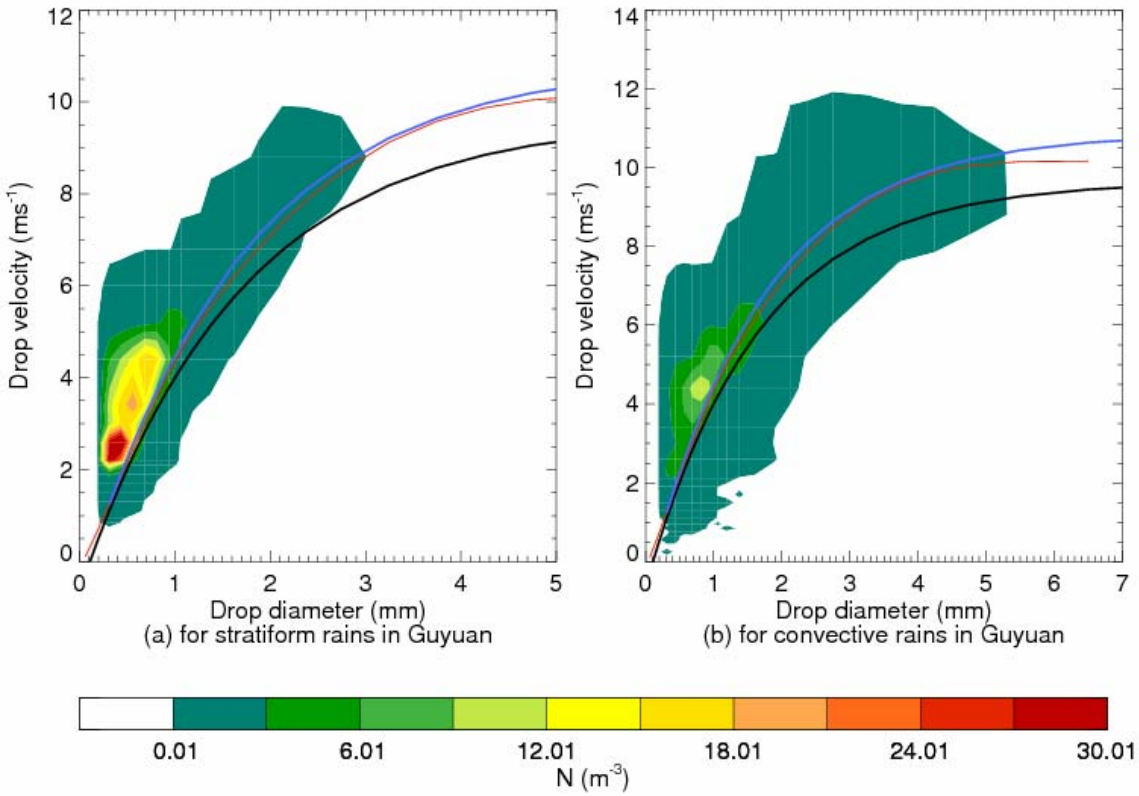
Drop velocity (ms-1)
Drop diameter (mm)
(a) for stratiform rains in Guyuan
Drop velocity (ms-1)
Drop diameter (mm)
(b) for convective rains in Guyuan
0.01
6.01
12.01
18.01
24.01
30.01
N (m-3)

Figure 9

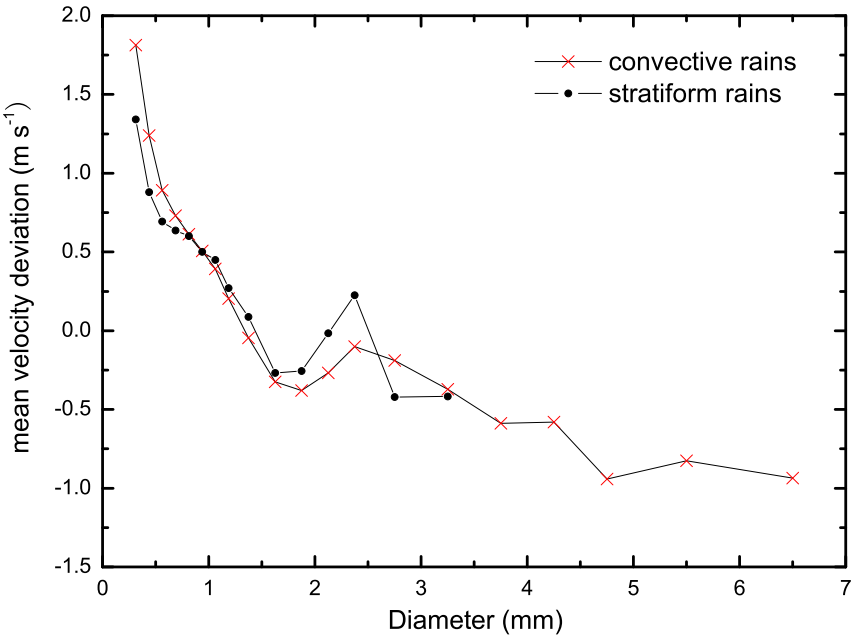
convective rains
stratiform rains
mean velocity deviation (m s-1)
Diameter (mm)
2.0
1.5
1.0
0.5
0.0
-0.5
-1.0
-1.5
0
1
2
3
4
5
6
7

Figure 10

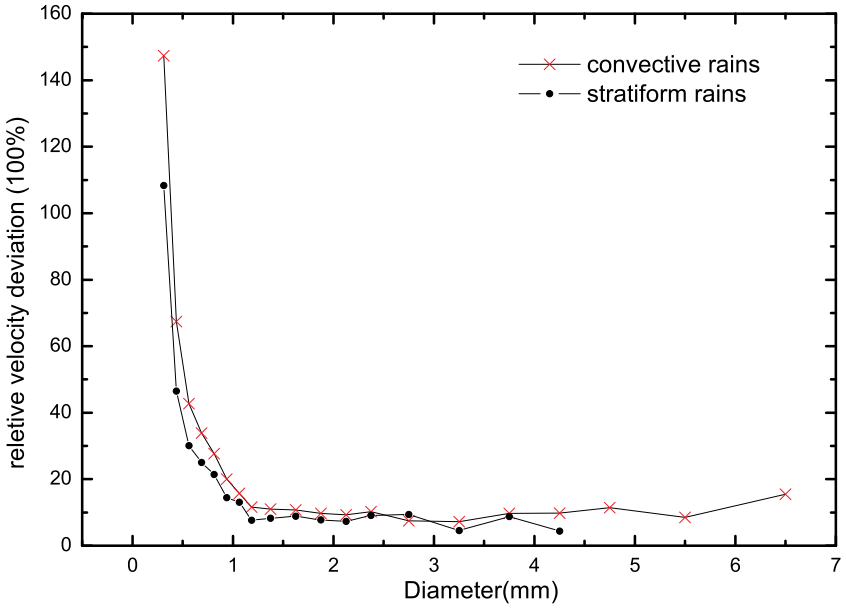
convective rains
stratiform rains
reletive velocity deviation (100%)
Diameter(mm)
0
20
40
60
80
100
120
140
160
0
1
2
3
4
5
6
7

Figure 11